

Rotation-vibration CARS spectra of the $2\nu_2$ mode in CO_2 gas^{a)}

C. M. Roland^{b)} and William A. Steele

Department of Chemistry, The Pennsylvania State University, University Park, Pennsylvania 16802
(Received 4 January 1980; accepted 30 January 1980)

Polarized and depolarized CARS band shapes are reported for the $2\nu_2$ band of the Fermi resonance diad in room temperature CO_2 gas at a series of densities. Analysis of the spectra yields vibrational relaxation times and the shift of the band center with density. Comparison of the depolarized spectra with the J diffusion model for reorientation shows that there is good agreement. Effective collision frequencies are obtained for various densities. The frequency shifts, the inverse vibrational relaxation time and the collision frequency are all linear functions of density except at the highest densities. Binary collision cross sections are calculated for angular momentum and for vibrational relaxation. The advantages of these and other CARS measurements relative to more conventional spectroscopies are briefly discussed.

I. INTRODUCTION

We have recently reported^{1,2} quantitative studies of intensities in vibration-rotation and pure rotation CARS bands for several liquids and vapors. Both polarized and depolarized spectra were measured using a standard three-color arrangement in which pulsed pump and Stokes laser beams with (angular) frequencies ω_1 and ω_2 , respectively, were focused together in the sample to generate a CARS beam with frequency $\omega_{as} = \omega_1 + \omega_2$, where $\omega = \omega_1 - \omega_2$. For a vibration-rotation band, the intensity $I_{\text{CARS}}(\omega)$ detected at ω_{as} can be calculated using the time-correlation function formalism by evaluating³

$$I_{\text{CARS}}(\omega) \propto N^2 \left| \int_0^\infty C(t) e^{-i\omega t} dt + iB \right|^2, \quad (1.1)$$

where N is the density and B is proportional to the electronic susceptibility χ^{NR4} :

$$B = \frac{\hbar\omega_2^4}{2Nc^4} (d\sigma/d\Omega)^{-1} \chi^{NR}, \quad (1.2)$$

where $(d\sigma/d\Omega)$ is the spontaneous Raman cross section. B is purely real in the absence of two-photon resonances.

The key to a successful interpretation of a measured spectrum is in the modeling of the vibration-rotation time-correlation function $C(t)$. Note that this function includes all sources of broadening of the vibrational resonance in the spontaneous Raman susceptibility, including instrumental effects as well as any collision-induced terms. Because the transform in Eq. (1.1) is squared, $C(t)$ cannot be directly obtained by Fourier transform of $I_{\text{CARS}}(\omega)$, as is commonly done in spontaneous Raman and infrared studies. It is necessary, rather, to assume some model for the dynamics of the system and then use the resulting $C(t)$ to generate theoretical CARS spectra which are then fitted to experiment by varying the available adjustable parameters.

Neglecting instrumental effects for the moment, the dynamical behavior of consequence for spectral bands such as those studied here is primarily coupled vibration

and rotational motion. Our previous investigation² of the Q -branch CARS spectrum for the stretching mode in nitrogen gas at various densities showed that vibration-rotation coupling was the primary source of bandwidth at low densities, giving easily resolved spectral lines at pressures of 1 atm or less. However, as the density of the gas or the moment of inertia go up, these vibration-rotation lines tend to collapse into a continuous band of width which would be considerably smaller than that due to relaxation in the vibrational degree of freedom. Vibration-rotation coupling will be neglected in this study so that we write

$$C(t) = C_{\text{inst}}(t) C_{\text{vib}}(t) C_{\text{rot}}(t), \quad (1.3)$$

$$C_{\text{vib}}(t) = \exp(-t/\tau_v) \exp(2\pi i \nu t), \quad (1.4)$$

where τ_v is essentially a dephasing time and ν is the frequency of the overtone of the ν_2 mode in the CO_2 molecule.

One advantage of CARS relative to spontaneous Raman is that the instrumental broadening is small or, to put it another way, it is difficult to achieve the resolution in a spontaneous Raman experiment that is routine in CARS. Specifically, it is the sum of the laser widths that determines the instrumental width in CARS. Actually, it is the root mean square for Gaussian laser frequency spectra,⁵ but this distinction is unnecessary in the present work. Given that this laser broadening amounts to $\sim 0.3 \text{ cm}^{-1}$, we simply define an effective τ'_v as the sum of the true τ_v plus the inverse of the instrumental half-width at half-maximum (HWHM)_i:

$$\tau'_v = [\tau_v^{-1} + 2\pi c (\text{HWHM})_i]^{-1}. \quad (1.5)$$

Both polarized and depolarized CARS spectra were measured in CO_2 at room temperature over a range of density from 0.004 to 0.3 times the critical density. The polarized spectra could be fitted by exponentially decaying vibrational correlation functions, and the depolarized bands, by products of vibrational and rotational correlation functions, with rotational dynamics that are modeled by the well-known J -diffusion model.⁶ This describes the motion as classical free rotation interrupted by impulsive collisions that randomize the angular momentum without altering the orientation. The fitting parameters for both vibrational and rotational correlation functions can be related to the collisional cross

^{a)}This work supported by a research grant and a departmental instrumentation grant from the National Science Foundation.

^{b)}Present address: Central Research Laboratories, Firestone Tire and Rubber Co., Akron, Ohio 44317.

sections for the randomization processes in each case. Numerical values for these parameters are reported and briefly discussed.

II. EXPERIMENTAL RESULTS

The Fermi resonance diad of ν_1 (symmetric stretch) and $2\nu_2$ (overtone bending) has been intensively investigated in CO₂ gas.⁷⁻⁹ Previous studies have shown that the band centered at 1389 cm⁻¹ is primarily $2\nu_2$, and the band at 1287 cm⁻¹ is primarily ν_1 . Since both of these modes have the same symmetry, the arguments concerning the effects of vibrational and rotational relaxation upon bandwidth should be similar. For convenience, we have studied the more intense of the two bands.

The experimental spectroscopic arrangement used in this work has been described in a previous paper.¹ A simple pressure cell was used to confine the CO₂ gas at room temperature. It consisted of a cylindrical brass container of 6 cm optical path length and internal diameter equal to 1.2 cm. Rubber O rings maintained the pressure-vacuum seal between the metal cell and 0.6 cm thick glass windows. A metal bourdon gauge mounted on the cell provided for pressure measurements up to 1000 psi. The only other significant modification of the apparatus described previously¹ was the use of a dichroic mirror to combine the pump and the Stokes beams preparatory to passing them into the sample. This simple arrangement was made possible by the fact that we are here working with laser frequencies ω_1 and ω_2 that differ by ~ 1400 cm⁻¹.

Polarized spectra of the $2\nu_2$ band were obtained at pressures ranging from 1–50 atm; typical bands are shown in Fig. 2. It was found that the contribution of nonresonant susceptibility to these bands could be neglected, and that the band shapes could be accurately fitted to the calculated spectra obtained when one ne-

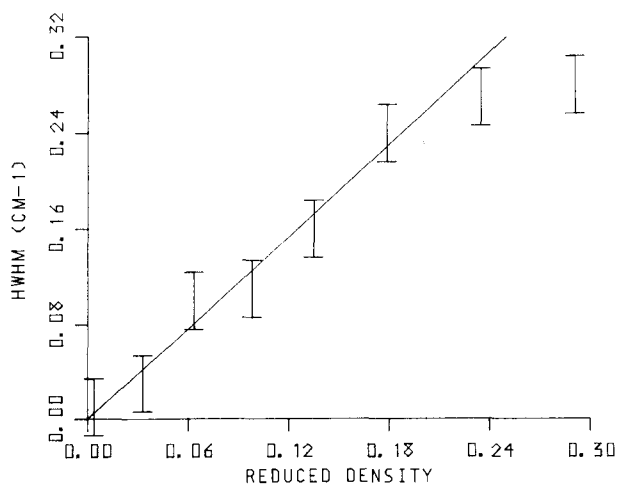


FIG. 1. The half-width at half-maximum of the polarized $2\nu_2$ CARS spectra of CO₂ are plotted as a function of N/N_{crit} , where N_{crit} is the critical density. An instrumental width of 0.27 cm⁻¹ has been subtracted from each data point. The estimated uncertainty is indicated. Except at the highest densities the points fall on a straight line, as would be expected for vibrational dephasing caused by binary collisions.

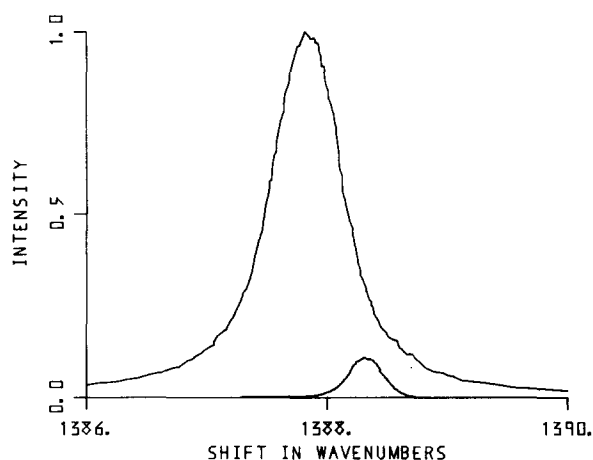


FIG. 2. Experimental curves of polarized spectra are shown here for two values of reduced density $\bar{p} = N/N_{\text{crit}}$. The weak spectrum is for $\bar{p} = 0.004$ (1 atm) and the intense one for $\bar{p} = 0.135$. The shift in peak with density is clearly indicated; since the contribution of the nonresonant background is negligible in these spectra, the peak intensities occur at $2\nu_2$, the vibrational frequency. Note also that the peak heights vary with $N^2 \tau_v'^2$, where $\tau_v' = [\tau_v^{-1} + 2\pi c(\text{HWHM})_i]^{-1}$. Since τ_v is inversely proportional to density N (see Fig. 1), one might expect the peak height to be independent of density. This is true at high density where the instrumental width is negligible; however, the observed spectra peak width at $\bar{p} = 0.004$ is almost entirely instrumental and thus the peak height is much smaller than the value predicted from $N^2 \tau_v'^2$.

glects the contribution of rotation and uses the exponential approximation to the combined vibrational and instrumental time-correlation function. In fact, if one writes $\tau_v' = 1/(\text{HWHM})$, a plot of experimental HWHM versus density gives a good straight line except at the highest densities, with an intercept of 0.27 cm⁻¹, which is the instrumental contribution to the linewidth. After subtraction of this intercept, the half-widths were plotted as shown in Fig. 1. The slope of the straight line is 5.2×10^{-3} cm⁻¹/amagat. As will be discussed below, a dephasing cross section can be extracted from these data. (However, it is possible that relaxation by vibrational energy level change is also important.) The deviation of the experimental points from linearity at high density may reflect the onset of motional narrowing; in effect, a partial averaging of the fluctuating force on the normal coordinate of a vibrating molecule occurs due to the presence of several collision partners at once.

Figure 2 shows quite clearly that the point of maximum CARS signal shifts with pressure. If the nonresonant susceptibility is negligible, the position of maximum intensity corresponds to $2\nu_2$. It was found that the shift was linear in density except at the highest values and amounted to -0.011 cm⁻¹/amagat. An uncertainty of 0.003 cm⁻¹/amagat arises partly from problems in locating the peak of the intensity and in part from problems in obtaining sufficiently precise frequency scans at 1390 cm⁻¹ displacement of the input lasers.

Since it appears that the shape of the polarized $2\nu_2$ spectrum is sensitive only to instrumental broadening and to purely vibrational relaxation, we also neglect

TABLE I. Parameters obtained from the fit of the CARS spectra to model calculations.

ρ/ρ_{crit}	τ_v (ps)	B_{dep} (ps)	β (ps ⁻¹)	τ_r (ps)	τ_J (ps)
0.064	63	0.077	0.16	1.58	6.3
0.099	42	0.070	0.26	1.07	3.8
0.139	30	0.070	0.43	0.74	2.3
0.183	23	0.074	0.53	0.61	1.9
0.233	18	0.070	0.72	0.50	1.4
~0.8	5	0.068	~1.3	~0.34	~0.8

Note: Rotational parameters are often reported in reduced units obtained by dividing time (or multiplying for frequency) by $\sqrt{I/kT}$. For CO₂ at 297°K, $\sqrt{I/kT}=0.421$ ps. Also, $N_{\text{crit}}=0.466$ g/cm³ (=239 amagat).

vibration-rotation interaction effects upon the time-correlation function $C_{\text{dep}}(t)$ for the depolarized spectrum and write

$$C_{\text{dep}}(t) = \exp(-t/\tau'_v)C_{\text{rot}}(t). \quad (2.1)$$

For $C_{\text{rot}}(t)$, we employ the J -diffusion model of Gordon.⁶ Since the collisional probabilities in this model are given by a Poisson distribution with a collision frequency β which is equal to the inverse of the angular momentum relaxation time, the only adjustable parameter is this collision frequency. At low to moderate pressures, β should be a linear function of density. The presence of the relatively rapid rotational relaxation gives rise to depolarized CARS spectra that are much broader than the polarized bands. Consequently, the contribution of the nonresonant electronic susceptibility to the observed intensity is no longer negligible compared to the resonant signal. To a first approximation, the magnitude of this electronic susceptibility is constant over the spectral range and scales linearly with the density. The areas under the time-correlation functions used here are normalized to a constant value:

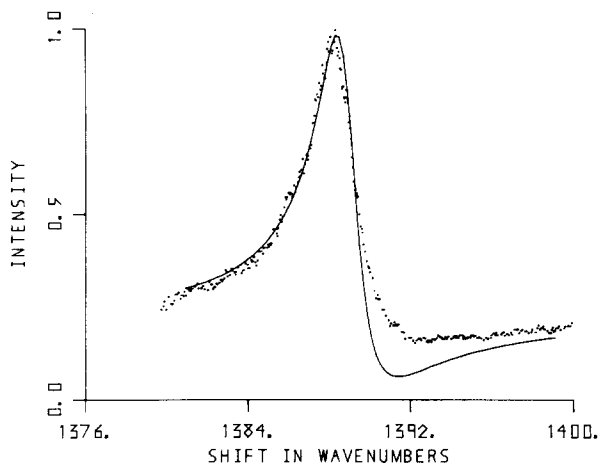


FIG. 4. Same as Fig. 3, but at $\bar{\rho}=0.099$ (pressure=326 psi); values of β and B_{dep} are listed in Table I for this and Figs. 5-8.

$$\int_{-\infty}^{\infty} \int_0^{\infty} C(t)e^{-i\omega t} dt d\omega = \pi C(0) = \pi \quad (2.2)$$

(in fact, the frequency limits extend only over the band of interest, but this causes no complications). Therefore, the values of the constant B used in Eq. (1.1) to fit theory to experiment should be independent of density. Except for minor adjustments made to optimize the fit, the values shown in Table I show that this was indeed the case, with an average $B_{\text{dep}}=0.72 \pm 0.02$ psec. Experimental depolarized spectra are compared with the optimized model calculations in Figs. 3-8. The agreement obtained is quite good, especially considering the sensitivity of calculated CARS band shapes to model.² We emphasize here that the choice of B_{dep} affects much more than the base line of the spectra; because of the cross term in Eq. (1.1) between the imaginary part of the transform of $C(t)$ and (the imaginary) iB_{dep} , an important part of the frequency dependence of these spectra comes from this factor. Only when $\omega = 2\pi\nu$ is the cross term absent from the CARS intensity; in contrast to the polarized spectra where background effects are negligible, this intensity is not necessarily maximum at this

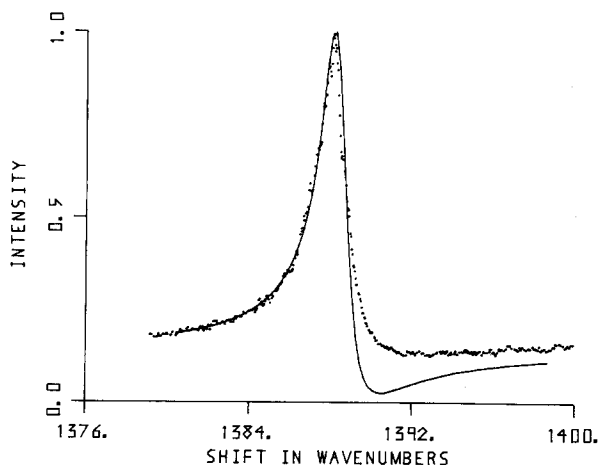


FIG. 3. Pepolarized CARS spectra of the ν_1 band of CO₂ at reduced density $\bar{\rho}=0.0643$. Under the experimental conditions (room temperature=24°C), the gas pressure is 223 psi. The points are experimental and the solid line is given by the J -diffusion model with $\nu \approx 1388$ cm⁻¹, $\beta=0.20$ ps, and $B_{\text{dep}}=0.077$ ps.

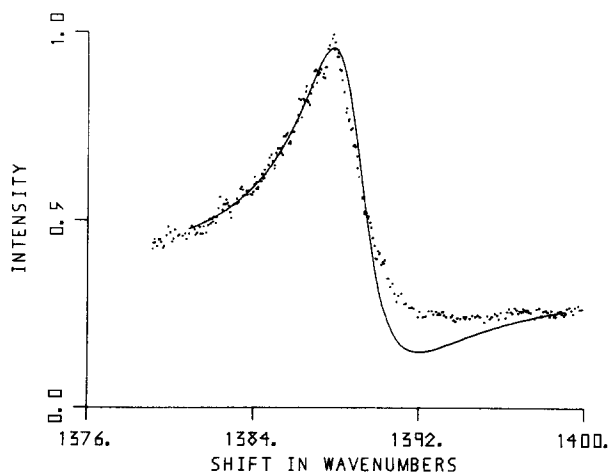
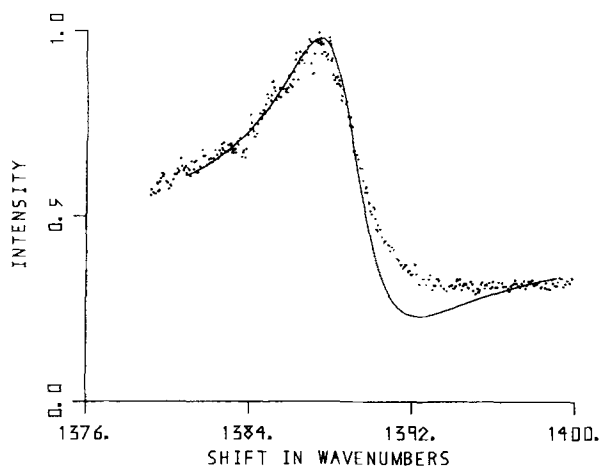


FIG. 5. Same as Fig. 3, at $\bar{\rho}=0.139$, $p=436$ psi.

FIG. 6. Same as Fig. 3, at $\bar{p}=0.183$, $p=537$ psi.

point. Nevertheless, it is of interest to note that fits of the calculated spectra to experiment indicate that ν for the depolarized spectra varies with density, but with essentially the same slope as the polarized band. It was found that $d\nu(\text{dep})/dN = -0.012 \text{ cm}^{-1}/\text{amagat}$. (Because these peaks are broader, it is more difficult to locate the positions of the maxima and thus the estimated uncertainty in the slope is $0.005 \text{ cm}^{-1}/\text{amagat}$.)

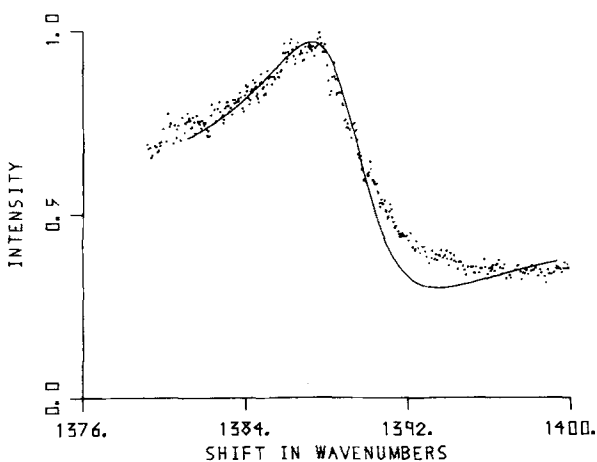
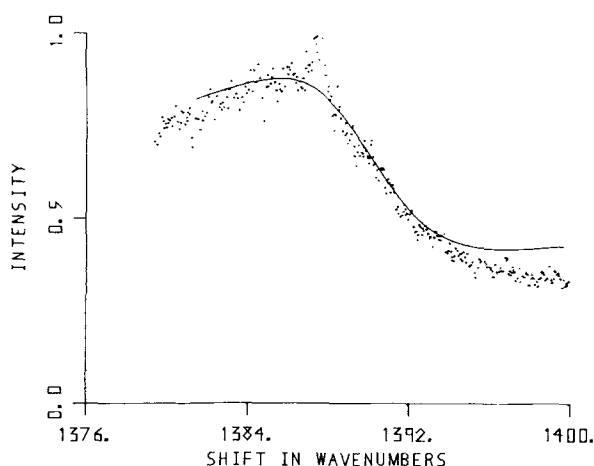
Since the resonant–nonresonant cross term is zero when $\omega = 2\pi\nu$, it is generally true that

$$I_{\text{CARS}}^{\text{dep}}(\nu) \propto N^2(\tau_{v-r}^{\prime 2} + B_{\text{dep}}^2), \quad (2.3)$$

where τ_{v-r}^{\prime} is the sum of the vibration–rotation correlation time τ_{v-r} and the instrumental term; for an exponentially decaying vibrational correlation and negligible vibration–rotation coupling, τ_{v-r} is thus given by

$$\tau_{v-r} = \int_0^{\infty} \exp(-t/\tau_v) C_{\text{rot}} dt. \quad (2.4)$$

It is well known that $C_{\text{rot}}(t)$ for the J -diffusion model can be expressed as a sum of convolutions of time integrals arising from $0, \dots, n$ collisions in the gas.⁷ We define the complex Laplace transform $\delta(q)$ by

FIG. 7. Same as Fig. 3, at $\bar{p}=0.233$, $p=637$ psi.FIG. 8. Same as Fig. 3, at $\bar{p} \approx 0.8$; $p=862$ psi.

$$\delta(q) = c(q) + i s(q) = \int_0^{\infty} \exp(iqt) C^{\text{tr}}(t) dt, \quad (2.5)$$

where $C^{\text{tr}}(t)$ is the free rotor correlation function [of $P_2(\cos\theta)$, the Legendre polynomial with argument $\cos\theta$, for the spectra of interest here]. The rotational correlation time $\tau_r(\beta)$ is given by

$$\tau_r(\beta) = \sum_{n=1}^{\infty} \beta^{n-1} \text{Re}[\delta(\beta)^n], \quad (2.6)$$

but the vibration–rotation correlation time for an exponential vibrational correlation function is equal to

$$\tau_{v-r}(\beta, \tau_v) = \sum_{n=1}^{\infty} \beta^{n-1} \text{Re} \left[\delta \left(\beta + \frac{1}{\tau_v} \right) \right] \quad (2.7)$$

$$= \frac{c \left(\beta + \frac{1}{\tau_v} \right)}{1 - \beta c \left(\beta + \frac{1}{\tau_v} \right)}. \quad (2.8)$$

(If the J -diffusion model is obeyed, this argument is valid for any vibration–rotation band, not just for CARS.) Of course, if τ_v is very large compared to $1/\beta$, the effect of vibrational relaxation can be neglected and $\tau_{v-r} \approx \tau_r$, as expected. More generally, the calculations of $\tau_r(\beta)$ that have been reported for the J -diffusion model can be used to evaluate Eq. (2.8) for the vibration–rotation correlation time. Equations (2.6) and (2.8) yield

$$\tau_{v-r}(\beta, \tau_v) = \frac{\tau_r(\beta')}{1 + \tau_v^{-1} \tau_r(\beta')}, \quad (2.9)$$

where $\beta' = \beta + \tau_v^{-1}$. Furthermore, values listed in Table I for the fitting parameters of both the polarized and depolarized bands indicate that the product $\tau_v^{-1} \tau_r(\beta')$ is roughly independent of density and equal to ~ 0.03 , under the conditions of these experiments. Also, $\beta' \approx 1.1\beta$. Since the nonresonant term B_{dep} defined in Eq. (1.2) is actually independent of density, the resonant/nonresonant intensity ratio (in the frequency region near the maximum) varies as $\tau_r(\beta')$. Several calculations of the dependence of the rotational correlation time upon collision frequency in the J -diffusion model^{10,11} show that τ_r first decreases with increasing β , then passes through

a maximum, and eventually becomes proportional to β . When the present experiments are fitted to this model, one finds that these correlation times decrease with increasing density and thus that they decrease with increasing β . The purpose of this analysis is to give some understanding of the manner in which the relative resonant/nonresonant intensity varies with density at frequencies near those corresponding to the peak value. It can now be seen that the J -diffusion model leads one to expect that the ratio will decrease with increasing density over the range of these experiments (as shown in Figs. 2–8), but also that it should begin to increase at even higher density. Of course, the trend in τ_r with density is not unique to the J -diffusion model; this behavior is expected in general.

In fitting theory to experiment, primary emphasis was placed on fitting near the peak of the CARS signal. A number of complicating factors are present which can account for lack of agreement in the wings. Not only is there intensity from the ν_1 member of the Fermi diad which thus produces a pair of lines in the spontaneous Raman spectrum at ~ 1388 and ~ 1285 cm⁻¹, hot bands associated with excited ν_2 levels give satellite lines appearing at ~ 1410 and ~ 1265 cm⁻¹. Contributions to the measured intensity from these neighboring resonances have been neglected here, as necessitated by the lack of intensity and depolarization data on the resonances as a function of density (the Fermi interaction is density dependent due to shift of the vibrational frequencies with density). The closest of these resonances is only 20 cm⁻¹ higher in frequency and is moderately intense in the polarized Raman spectrum ($\sim 1/15$ of $2\nu_2$, at 1 atm).⁹ Qualitatively, the effect of this blue-shifted neighboring band arises mainly because of the cross term between the imaginary susceptibility component $\chi''_{\nu_2}(\omega)$ and the corresponding imaginary part $\chi''_{\nu_1}(\omega)$ for ν_1 . One defines

$$\chi''_{\nu}(\omega) \propto - \int_0^{\infty} C_{\nu}(t) \sin \omega t dt. \quad (2.10)$$

In the wings of the $2\nu_2$ band where χ_{ν_1} is small, a term appears in $I_{\text{CARS}}(\omega)$ that depends upon $\chi''_{\nu_1}(\omega)[B_{\text{dep}} + \chi''_{2\nu_2}(\omega)]$. It is interesting to note that this term changes sign as density is varied. For ω positive (frequencies greater than 1390 cm⁻¹), $\chi''_{2\nu_2}(\omega)$ is negative and thus there is partial cancellation with the positive B_{dep} . At the lowest densities, the resonant susceptibility is sharply peaked and B_{dep} dominates at large ω (i.e., greater than 10 cm⁻¹ shifted from the central frequency). Since $\chi''_{\nu_1}(\omega)$ is also positive at these frequencies, the neglected term gives rise to added intensity in the calculated spectra. [Of course, a negative contribution to the intensity is expected at frequencies less than 1390 cm⁻¹, but this will be quite small because $\chi''_{\nu_1}(\omega)$ decreases as one goes further from the central ν_1 at 1410 cm⁻¹.] As density increases, both resonant bandwidths increase, and $\chi''_{2\nu_2}(\omega)$ thus becomes more negative for frequencies near 1400 cm⁻¹. Eventually, the resonant susceptibility in this frequency region overwhelms the positive B_{dep} term. The neglected contribution to the susceptibility then becomes negative and consequently a sign change in the discrepancy between experiment and theory is expected

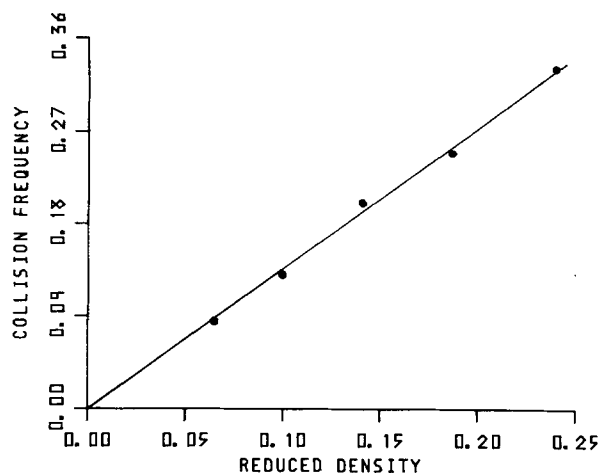


FIG. 9. Reduced collision frequency $\beta^* = \beta\sqrt{1/kT}$ obtained from fits of experiment to J -diffusion model is plotted versus reduced density N/N_{crit} .

(and observed in Fig. 8).

We have neglected collisionally induced polarizability distortions in our calculations of both the polarized and depolarized spectra. Crude estimates of the importance of this contribution to the depolarized light scattering spectra of liquid CO₂ indicate that it amounts to only 10% of the total scattered intensity even at densities an order of magnitude higher than those used in the present study.^{12,13}

The high density spectrum shown in Fig. 8 is included for comparison with the other curves, but has not been included in the data analysis. It suffers from several experimental difficulties related primarily to proximity to the critical point of CO₂. First, the strong p , T dependence of density in this region makes it difficult to obtain an accurate estimate of the density; second, large density fluctuations are present that give rise to significant opalescence and a fluctuating CARS signal; and third, this experiment happens to be at a density with a collision frequency β that corresponds to the minimum in τ_r , and consequently the spectrum is quite wide, has a weak maximum, and is more obscured by the nonresonant background intensity.

Densities for each of the spectra measured are given in Table I together with the best-fit collision frequencies and orientational correlation times. In the J -diffusion model, all correlation in angular momentum is lost when a collision occurs so that the collision frequency is just the inverse of τ_J , the angular momentum correlation time and also the decay time in the angular momentum correlation function.

Both the collision frequencies and the vibrational relaxation times can be utilized to extract cross sections Σ for the appropriate relaxation process. For example, if we temporarily neglect the nonsphericity of the CO₂ molecule,^{14,15}

$$\beta = 4 \sqrt{\frac{kT}{\pi m}} \rho g(\sigma) \Sigma, \quad (2.11)$$

TABLE II. Effective collision frequencies for liquid CO₂ compared with extrapolated gas phase values.

N/N_{crit}	$\beta^* = \beta\sqrt{T/kT}$		Ratio
	From depolarized light scattering ¹¹	From gas phase CARS	
1.6	4.0	1.9	2.1
2.0	6.0	2.4	2.5
2.2	8.0	2.6	3.1

where $g(\sigma)$ is equal to the correlation function for a pair of hard spheres of diameter σ in contact and ρ is the density of the fluid. For the densities used here, negligible error is made in setting $g(\sigma) = 1$. The plot of β versus N/N_{crit} in Fig. 9 shows that the fitted collision frequencies are linear in density. From the slope in Fig. 9, one can calculate Σ_r , the cross section for angular momentum relaxation, to be 84 Å². This value is noticeably larger than the cross section obtained from viscosity (50 Å²)¹⁶ or from van der Waal's constants (32 Å²). This finding is easy to rationalize by noting that large changes in angular momentum occur when the ends of a pair of long linear molecules strike each other. Such occur for trajectories with large center-of-mass impact parameters—large enough so that translational momentum changes will be relatively small. It is interesting to note that molecular shape actually enters through the torques that control angular momentum changes. In highly symmetric molecules (such as tetrahedra), these torques are small compared to those for linear symmetry. Estimates of angular momentum relaxation times for symmetrical molecules¹⁷ yield angular momentum cross sections that are actually smaller than those from viscosity or van der Waal's constants.

A cross section for vibrational dephasing can also be estimated from the observed linear variation of τ_v^{-1} with density. One merely replaces β in Eq. (2.11) with the inverse of τ_v to find a cross section $\Sigma_v = 7.5$ Å². This small value clearly reflects the fact that it is more difficult to perturb the vibrational motion than either the rotational or the translational momentum in a collision.

Previous measurements^{13,18} of the depolarized light scattering from CO₂ at liquid densities have been fitted to the J -diffusion model to yield values of β . Although the fit is far from perfect and the J -diffusion description of molecular rotation is of dubious validity for liquids, we nevertheless can compare these values with the β given by a linear extrapolation of present results to high densities. Table II shows the results of this calculation; it is tempting to conclude that the "collision frequencies" in the liquid are enhanced because the development of short range order at high density gives effective $g(\sigma)$ that are significantly larger than unity.

III. DISCUSSION

From the results presented here, together with previous studies from our laboratory,^{1,2} it is evident that useful quantitative information can be obtained from

analysis of CARS band shapes in dense gases and in simple liquids. In principle, the same information can be obtained from spontaneous Raman spectra. In practice, the need for high resolution and problems of interpretation when the spectra contain overlapping bands means that it may be difficult or even impossible to use spontaneous Raman in this way. Indeed, the systems chosen in our work (gaseous CO₂ and N₂, and liquid CCl₄ and CH₃I) have been very extensively studied by other spectroscopic techniques. In addition to confirming and refining some previously known parameters, we extracted new and useful data from the CARS spectra. For example, in the present study alone, both vibrational and orientational collision cross sections have been extracted from the experiment; estimates of the shift in $2\nu_2$ due to binary collisions have also been made for both polarized and depolarized spectra. We note in passing that these estimates could be considerably refined if experiments were specifically designed to measure them by differential measurements of CARS spectral peak positions for low and high density.

The fact that comparison of CARS spectra with models must be done by trial and error rather than by Fourier transform of the data and then comparison with model time-correlation functions is no more than an inconvenience. Indeed, in careful analyses of Raman or infrared data, a variety of corrections for instrumental broadening, collision-induced intensity, neighboring bands, etc. must be applied to the raw data, either before or after Fourier transforming. We find that the first two of these correction factors are less important in CARS than in spontaneous Raman; instrumental width can be made smaller with less effort in CARS and collision-induced effects are smaller because they generally amount to a small fraction of the Raman susceptibility (0.1–0.3), which is then squared to give the CARS intensity. On the other hand, the presence of neighboring bands can give rise to severe problems in interpreting band shapes in either spectroscopy.

Wright and Wang⁸ have reported polarized and depolarized spontaneous Raman measurements of the density dependence of $2\nu_2$ and have concluded that both types of spectra give

$$2\nu_2 = 1389.1 - 0.0053\rho \text{ (cm}^{-1}\text{)},$$

with the density ρ ranging up to ~ 500 amagat. This result disagrees somewhat from the high resolution Raman⁷ and the CARS results, which can be summarized as

$$2\nu_2 = 1388.3 - 0.011\rho.$$

Since analysis of the high resolution infrared bands suggests that $2\nu_2 = 1388.17 (\pm 0.03)$ cm⁻¹ at low density⁷ and since our measurements are made at higher resolution than those of Wright and Wang, it would seem that the CARS results for the slope are more reliable. However, the difference in the two values obtained for the slope is of the same order of magnitude as the combined uncertainties (equal to ± 0.004 cm⁻¹/amagat in our work, but not given by Wright and Wang). A possible explanation for the discrepancy is the presence of an unresolved Q branch on the low frequency side of $2\nu_2$ that will have

different effects upon the line shape (and "central" frequency) in the spontaneous Raman and in the CARS experiments. We have not attempted a quantitative test of this hypothesis due to lack of knowledge of the appropriate vibration-rotation coupling constant.

Experimentally, we have demonstrated in this and in the previous papers that polarized and depolarized CARS intensities can be measured reproducibly and accurately over the ranges of frequency needed to characterize many pure rotation or vibration-rotation bands. Thus, we conclude that CARS can be a useful supplement to spontaneous Raman or infrared experiments, and that it is capable of yielding information concerning band positions and widths that is often difficult to obtain in alternative spectroscopies, particularly when the bands are narrow or are made up of discrete but closely spaced lines.

¹C. M. Roland and W. A. Steele, *J. Chem. Phys.* **73**, 5919 (1980).

²C. M. Roland and W. A. Steele, *J. Chem. Phys.* **73**, 5924 (1980).

³J. O. Bjarnason, B. S. Hudson, and H. C. Andersen, *J. Chem. Phys.* **70**, 4130 (1979).

⁴See, for example, J. W. Nibler, W. M. Shaub, J. R. McDonald, and A. B. Harvey, in *Vibrational Spectra and Struc-*

ture, edited by J. R. Durig (Elsevier, New York, 1978), Vol. 6.

⁵M. A. Yuratich, *Mol. Phys.* **38**, 626 (1979).

⁶R. G. Gordon, *J. Chem. Phys.* **44**, 1830 (1966).

⁷H. E. Howard-Lock and B. P. Stoicheff, *J. Mol. Spectrosc.* **37**, 321 (1971); C. P. Courtoy, *Can. J. Phys.* **35**, 608 (1957); G. Amat and M. Pimbert, *J. Mol. Spectrosc.* **18**, 278 (1965); H. R. Gordon and T. K. McCubbin, Jr., *J. Mol. Spectrosc.* **19**, 137 (1966).

⁸R. Wright and C. H. Wang, *J. Chem. Phys.* **58**, 2893 (1973); C. H. Wang and R. B. Wright, *Chem. Phys. Lett.* **23**, 241 (1973).

⁹H. L. Walsh, P. E. Pashler, and B. P. Stoicheff, *Can. J. Phys.* **30**, 99 (1952).

¹⁰W. A. Steele, *Adv. Chem. Phys.* **34**, 1 (1976).

¹¹R. E. D. McClung, *J. Chem. Phys.* **57**, 5478 (1972).

¹²D. Frenkel and J. P. McTague, *J. Chem. Phys.* **72**, 2801 (1980).

¹³P. van Konynenburg and W. A. Steele, *J. Chem. Phys.* **62**, 2301 (1975).

¹⁴D. Enskog, *K. Sven. Vetenskapsakad. Handl.* **64**, (1922).

¹⁵T. Einwohner and B. J. Alder, *J. Chem. Phys.* **49**, 1458 (1968).

¹⁶J. O. Hirschfelder, C. F. Curtiss, and R. B. Bird, *Molecular Theory of Gases and Liquids* (Wiley, New York, 1954).

¹⁷A. A. Maryott, M. S. Malmberg, and K. T. Gillen, *Chem. Phys. Lett.* **25**, 169 (1974).

¹⁸M. Perrot, J. Devaure, and J. Lascombe, *Mol. Phys.* **30**, 97 (1975).